DEVELOPMENT AND EVALUATION OF SELENIUM NANOPARTICLES CONJUGATED SCAFFOLDS FOR CARDIAC TISSUE ENGINEERING APPLICATIONS

A SYNOPSIS

Submitted by

NAVEENKUMAR S
(Reg. No. 201901159)

In partial fulfillment for the award of the degree
Of
DOCTOR OF PHILOSOPHY

DEPARTMENT OF BIOTECHNOLOGY
SCHOOL OF BIO, CHEMICAL AND PROCESSING ENGINEERING
KALASALINGAM ACADEMY OF RESEARCH AND EDUCATION
(DEEMED TO BE UNIVERSITY)
ANAND NAGAR, KRISHNANKOIL – 626 126
TAMIL NADU, INDIA

JULY 2024

1. Introduction

In the context of advancing social and economic development, a global surge in alcohol consumption has given rise to significant challenges. Alcohol consumption has long been associated with various cardiovascular complications, including myocardial tissue damage. Chronic and excessive alcohol intake can lead to a spectrum of cardiac pathologies, ranging from cardiomyopathy to arrhythmias and heart failure. The mechanisms underlying alcohol-induced heart tissue damage are multifactorial, involving oxidative stress, inflammation, mitochondrial dysfunction, and alterations in cardiac gene expression. Despite advances in understanding these mechanisms, the precise pathways through which alcohol exerts its harmful effects on the heart remain incompletely elucidated. Moreover, the clinical implications of alcohol-induced cardiac damage extend beyond the individual immediate health, contributing to the global burden of cardiovascular diseases [1].

In recent years, the development of biomaterials with multifunctional properties has garnered significant attention in the field of medical research. Among these, injectable hydrogel comprising biopolymers are versatile matrices with promising applications in drug delivery, tissue engineering, and regenerative medicine. The intriguing aspect of these materials is their potential to exhibit antioxidant properties, which are crucial for mitigating oxidative stress-related damage in various biological systems. Oxidative stress, arising from an imbalance between the production of reactive oxygen species (ROS) and the antioxidant defense mechanisms, is implicated in numerous pathological conditions, including inflammation, neurodegenerative diseases, and aging [2]. Therefore, the development of antioxidant therapies holds immense therapeutic potential in combating these ailments.

The present study explores the development and potential applications of injectable hydrogels containing natural polymers like sodium alginate and pectin in conjunction with selenium nanoparticles (SeNPs). These hydrogels hold considerable promise for addressing alcohol-induced tissue damage, presenting innovative solutions for tissue engineering, drug delivery, and regenerative medicine.

2. Review of literature

2.1. Alcoholic Cardiomyopathy

Alcoholic cardiomyopathy (ACM) is a unique disease and more familiar to physicians as "alcoholic heart disease," coined by William Mackenzie. Alcohol addiction exists in most societies. "Tubingen Wine Heart," described in 1877 and "Munich Beer Heart," reported by German pathologist Otto Bollinger, are two popular references to harmful consequences of alcohol intemperance identified during the early 20^{th} century (George and Figueredo [3]) . The progression of alcoholic cardiomyopathy is initiated by alcohol addiction. Alcohol-induced damage in the heart reduces blood pumping and increases myocardial apoptosis (Piano [4]). In the latter half of the twentieth century, they witnessed a large meta-analysis of 34 studies comprising >1 million subjects and 10,000 deaths (Kloner and Rezkalla [5]). In an epidemiology study of women and men (490,000) in the middle age group, population group mortality increased with heavier drinking induced the risk of coronary heart diseases and stroke, including increased fibrinolysis, high-density lipoprotein (HDL) cholesterol, decreased fibrinogen, and reduced plasma viscosity and decreased platelet aggregation (Kuppari [6]). Alcoholic patients deformed in the cardiac structure and function change report consuming >90 g/d of alcohol for >5 years. It is imperative to note potential damage to the heart with long-lasting alcohol. Long-term studies have been conducted in rats that were fed 25 % alcohol solution for seven months. The ventricular contractile force was decreased after four months of study. Controls remain normal and myocardial depression was identified in the rat-administrated vitamin supplementation. Recently, another study was conducted on rats fed an isocaloric liquid diet. During the study period (10 months), rats were fed 39 % of the isocaloric liquid diet of their daily calories. Alcohol has been affecting the myocardium's function and structure. A few studies also reported that increased myocyte loss was observed due to apoptosis when the hearts were exposed to a high amount of alcohol. Ethanol and its metabolites are toxic to the myocyte, and unfavorable impacts were identified in cardiac myofibril shortening and myoprotein composition. Echocardiographic showed few abnormal functions, such as a decrease in fractional abnormalities, increased left atrial dimension,

and left ventricular wall thickness in heavy alcohol drinkers (Bär et al. [7]). Several researchers showed constant systolic dysfunction. The diastolic and systolic malfunctions have been seen in alcoholic cardiomyopathy in animal and human studies. The patient who has alcoholic cardiac myopathy also develops magnesium deficiency in the blood serum. A lower amount of magnesium reduction was observed in the blood when the patient's blood ethanol levels were above 80 mg/dL. These lead to cause arrhythmias and oxygen desaturation in the alcoholic patient (Brown et al. [8]).

2.2. Current Treatment Strategies for ACM

The management of alcoholic cardiomyopathy primarily focuses on abstinence from alcohol, lifestyle modifications, and pharmacological interventions aimed at symptom control and prevention of disease progression. However, the efficacy of existing treatment modalities in reversing alcohol-induced cardiac damage and restoring myocardial function remains limited (Ihekire et al. [9]). Pharmacological agents such as angiotensin-converting enzyme (ACE) inhibitors, beta-blockers, and aldosterone antagonists are commonly prescribed to manage heart failure symptoms and improve survival in patients with ACM. Nevertheless, these medications primarily target neurohormonal pathways and hemodynamic abnormalities associated with heart failure rather than addressing the underlying molecular mechanisms of alcohol-induced myocardial injury (Grunvald et al. [10]).

Surgical interventions such as cardiac transplantation may be considered in advanced cases of ACM refractory to medical therapy. However, the availability of donor organs, the risks associated with immunosuppressive therapy, and the long-term prognosis post-transplantation pose significant challenges in the management of ACM. Consequently, there is a critical need to develop innovative therapeutic approaches to promote myocardial regeneration, attenuate fibrosis, and restore cardiac function in individuals with ACM.

2.3. Hydrogel-Based Therapies for Cardiac Regeneration

Hydrogels represent a promising class of biomaterials for tissue engineering and regenerative medicine applications due to their biocompatibility, tunable properties, and ability to encapsulate bioactive molecules. Hydrogel-based scaffolds offer a three-dimensional microenvironment that mimics the native extracellular matrix (ECM) of cardiac tissue, providing structural support and facilitating cell adhesion, proliferation, and differentiation (Ho et al. [11]). Moreover, hydrogels can serve as reservoirs for the sustained release of therapeutic agents, growth factors, and stem cells, enhancing their regenerative potential in damaged cardiac tissue.

Several studies have explored the use of hydrogel-based formulations for cardiac repair and regeneration in preclinical models of myocardial infarction, ischemic heart disease, and heart failure. Hydrogels derived from natural polymers such as alginate, collagen, gelatin, and hyaluronic acid have been extensively investigated for their ability to promote angiogenesis, reduce scar formation, and improve cardiac function post-injury. Furthermore, the incorporation of bioactive components such as growth factors (e.g., vascular endothelial growth factor, fibroblast growth factor) and extracellular matrix proteins (e.g., laminin, fibronectin) into hydrogel matrices has been shown to enhance their therapeutic efficacy in cardiac tissue repair.

3. Objectives

- To synthesize, characterize and evaluate the cytotoxicity of selenium nanoparticles (SeNPs) encapsulated with sodium alginate, pectin and BSA in C2C12 cell lines.
- To prepare and characterize biocompatible alginate-pectin-SeNPs scaffold and investigate the alginate-pectin-SeNPs scaffold attachment in C2C12 cell lines.
- To characterize Chitosan-Collagen-SeNPs scaffold and in vitro assessment in C2C12 cell lines.
- To study the effect of alginate-pectin-SeNPs hydrogel in ethanol-induced mice.

4. The research gap

Sodium alginate-pectin-selenium nanoparticles hydrogel attenuated cardiac injury in a mice model" highlights the scarcity of comprehensive investigations into hydrogel-based therapies for mitigating cardiac injury in animal models. Existing therapies may have limitations, prompting the need for novel cardioprotective agents like selenium nanoparticles incorporated into hydrogel matrices to enhance treatment efficacy while minimizing adverse effects. Despite promising preclinical results, gaps persist in understanding the precise mechanisms by which the hydrogel formulation interacts with cardiac tissue and modulates cellular signaling pathways to attenuate injury progression. Bridging the gap between preclinical findings and clinical translation remains challenging, requiring further research to address safety, scalability, and regulatory approval hurdles. Additionally, optimizing the hydrogel's formulation parameters and delivery strategies is essential to maximize therapeutic benefits and minimize potential side effects, advancing its potential as a promising intervention for cardiac injury.

5. Materials and Method

5.1. Synthesis of SeNPs

Sodium selenite (0.2 mg) was dissolved in ascorbic acid (0.3 mg) in distilled water, stirring with a magnetic stirrer overnight. The above solutions were centrifuged at 10,000 rpm for 10 min, and the pellets were collected and stored

5.1.1. Synthesis of BSA-SeNPs

For the synthesis, 0.2 g of Sodium Selenite was prepared and mixed with 0.3 g of ascorbic acid, and 5 ml of BSA solution was mixed in a magnetic stirrer for 12 hrs. The obtained mixture was centrifuged 3 to 4 times at 10,000 rpm for 8-10 minutes, and the pellet was stored for further studies.

5.1.2. Synthesis of SA-SeNPs

For decoration purposes, sodium alginate (0.1 % wt/vol) was prepared and stirred for an hour to mix with sodium selenite (0.2 mg) and ascorbic acid (0.3 mg). This solution was kept in a magnetic stirrer overnight after being centrifuged at 10,000 rpm for 10 min.

5.1.3. Synthesis of PET-SeNPs

For decoration purposes, pectin was prepared (0.1 % wt/vol) and stirred for an hour to mix with sodium selenite (0.2 mg) and ascorbic acid (0.3 mg). This solution was kept in a magnetic stirrer overnight after being centrifuged at 10,000 rpm for 10 min.

5.2. Preparation of Alginate-Pectin (AP) scaffolds

Sodium Alginate (0.75 g) was dissolved in 1% of pectin (50 ml) and stirred for 1 hour. With this, added 7% glycerol. After that, the mixture was transferred to room temperature for 24 hrs for drying. The obtained scaffold was kept at -80°C for 24 hrs and neutralized with 5% calcium chloride for 20 minutes to get the hydrogel scaffold and air-dried. The same methodology was followed for preparing the Alginate-Pectin scaffold without SeNPs. The same method was followed to prepare the Alginate-Pectin scaffold with BSA-SeNPs, SA-SeNPs, and PET-SeNPs.

5.3. Preparation of CCS scaffold

Chitosan (1.5%) was dissolved in distilled water and stirred for 1 hour. To this solution, and 15% of glycerol was added and stirred. The mixture was instantly transferred onto a petri plate and dried for 24 hrs. Afterward, scaffolds were frozen at -80ºC overnight and neutralized with ~5% NaOH for 45 minutes. Finally, the scaffolds were washed with deionized water and air-dried. The same procedure was followed for preparing the CCS scaffolds with BSA-SeNPs, SA-SeNPs and PET-SeNPs.

5.4. Preparation of AP hydrogel

In 1.5% sodium alginate, distilled water was dissolved, with an additional 1% of pectin added and stirred for 1 hour. To this mixture, 15% glycerol was added. The resulting

mixture was stirred for 44 hours, and the obtained injectable hydrogel was then stored at -20°C for further study. The same methodology was followed for preparing the Alginate-pectin hydrogel with BSA-SeNPs, SA-SeNPs and PET-SeNPs.

5.5. Characterization Studies of SeNPs, BSA-SeNPs, SA-SeNPs and PET-SeNPs

The spectra of all the nanoparticles were examined using UV-vis spectrophotometry Thermo Scientific Evolution 201, with a wave range of 200 –800 nm. The scan speed of the sampling interval was 0.1min. The Fourier Transform Infrared spectrophotometer (FTIR) techniques, specifically the IR TRACER 100 model. The X-ray diffraction patterns of the nanoparticles were examined using an XRD (X-ray Diffraction) system, specifically the D8 Advance ECO XRD by Bruker, USA. The morphology analysis of the nanoparticles was investigated using a scanning electron microscope (SEM) from Carl Zeiss, specifically the EVO 18 model, in Germany. The Energy Dispersive X-ray Spectrometer (EDAX APEX) was used to study the elemental composition of nanoparticles. The size and zeta potential were determined by using DLS (HORIBA, SZ-100). An aliquot of 1 mL SeNPs, BSA-SeNPs, SA-SeNPs and PET-SeNPs solution, prepared in deionized water, was transferred to a polystyrene cuvette and tested at 25°C separately.

5.5.1. Characterization of AP, AP-BSA-SeNPs, AP-SA-SeNPs, AP-PET-SeNPs scaffolds, CCS, CCS-BSA-SeNPs, CCS-SA-SeNPs and CCS-PET-SeNPs scaffolds

This study examined all the scaffolds using Fourier Transform Infrared spectrophotometer (FTIR) techniques, specifically the IR TRACER 100 model. The X-ray diffraction patterns of the scaffolds were examined using an XRD, specifically the D8 Advance ECO XRD, by Bruker, USA. The morphology analysis of the scaffolds was investigated using a scanning electron microscope (SEM) from Carl Zeiss, specifically the EVO 18 model, in Germany. The TGA analysis of the scaffolds was conducted using a TGA (Thermogravimetric Analyzer) system, specifically the STA 800 Simultaneous Thermal Analyzer from PerkinElmer. The examination was performed over a temperature range from 50°C to 500°C, with a heating rate of 10°C per minute, all under a nitrogen atmosphere. The mechanical characteristics of the scaffolds were assessed

using a texture analyzer, specifically the Tex Pro TA10. The elongation rate was calculated employing the following formula:

$$\boldsymbol{\varepsilon = \frac{\Delta L}{L} X100}$$

Where,

Lo – The original gage length

ΔL – The change in length after subjecting the material to tensile stress and causing a fracture

5.6. Antioxidant activity assay

The antioxidant activity of SeNPs, BSA-SeNPs, SA-SeNPs, and PET-SeNPs, AP, AP-BSA-SeNPs, AP-SA-SeNPs, and AP-PET-SeNPs scaffolds, CCS, CCS-BSA-SeNPs, CCS-SA-SeNPs, and CCS-PET-SeNPs scaffolds, as well as AP, AP-BSA-SeNPs, AP-SA-SeNPs, and AP-PET-SeNPs hydrogel, was tested using DPPH assay method. The wavelength was recorded at 517 nm and measured with a UV-vis spectrometer (SHIMADZU UV-1800). DPPH (0.1 mM) was prepared and dissolved in methanol. 3 ml of DPPH solution was added to 1 ml of AP, AP-BSA-SeNPs, AP-SA-SeNPs, AP-PET-SeNPs hydrogels, SeNPs, BSA-SeNPs, SA-SeNPs and PET-SeNPs and to 1 mg of AP scaffold, AP-SeNPs scaffolds, CCS scaffold, and CCS-SeNPs scaffolds. The mixture was thoroughly vortexed and then incubated for 30 minutes in a dark room. Absorbance was measured at 517 nm. The following formula was used to evaluate the degradation of DPPH.

$$\boldsymbol{\%\ of\ SCV} = \frac{AB - AS}{AB} X100$$

Where,

AB is the absorption of the blank (DPPH + methanol)

AS is the absorption of the sample (DPPH + Methanol +Sample)

5.7. Cell culture

The C2C12 cell line was obtained from the National Centre for Cell Sciences (NCCS), Pune, India. Dulbecco's Modified Eagle Medium (DMEM) cells were maintained at 10%, and Fetal Bovine Serum (FBS) cells were grown at 5% CO_2 with 95% humidity at 37^{o}C.

5.8. MTT Assay

The C2C12 cells were seeded in a 96-well plate for 24 hrs at 37^{o}C in a CO_2 incubator. Then, cells were incubated with various concentrations of SeNPs (10, 20, 30, 40, and 50 µg/ml) for 72 hrs. After treatment, the medium was aspirated, and 10µL of fresh 0.1 mg/ml MTT solution was added into the wells. After incubation at 37^{o}C for 3 hrs, the medium changed color. To the medium, 100 µL of DMSO was added to each well. The plate was incubated at 37^{o}C under orbital shaking for 15 min, and the absorbance at 570 nm was measured using an Enspire Multimode plate reader (Perkin Elmer). MTT assay was performed in triplicate for each experiment. The percentage of cytotoxicity is calculated using the following formula:

$$\% \text{ of cytotoxicity} = 100 \text{ x } (\text{Control} - \text{Sample})$$

5.9. Preparation for *in vitro* tests

In the present study, the scaffolds' biocompatibility was checked by *in vitro* tests, including cell proliferation, cell morphology, and cell attachment in the C2C12 cell line. The AP, AP-BSA-SeNPs, AP-SA-SeNPs, AP-PET-SeNPs scaffolds, CCS, CCS-BSA-SeNPs, CCS-SA-SeNPs and CCS-PET-SeNPs scaffolds were washed with sterile PBS containing 500 U/mL penicillin and 500 µg/mL streptomycin, then sterilized at 121 °C for 20 minutes. The C2C12 cell line, sourced from the National Center for Cell Science (Pune, India), was cultured in DMEM supplemented with 10% fetal bovine serum, 100 U/mL penicillin, and 100 µg/mL streptomycin. Cells were maintained at 37 °C in a 5% CO_2 environment with ~95% humidity. Before the experiment, cells were trypsinized and re-suspended in DMEM with 10% FBS, 100 U/mL penicillin, and 100 µg/mL streptomycin. A 15 µL aliquot of the cell suspension (4.2×10^{-5} cells/mL) was added to each scaffold and incubated at 37 °C for 48 hrs.

5.10. Propidium Iodide (PI) staining

The C2C12 cells were fixed on the AP, AP-BSA-SeNPs, AP-SA-SeNPs, AP-PET-SeNPs scaffolds, CCS, CCS-BSA-SeNPs, CCS-SA-SeNPs and CCS-PET-SeNPs scaffolds using 3% paraformaldehyde and incubated for 20 min. Following incubation, the scaffolds

were washed with ice-cold PBS (pH 7.5) and stained with 50 mg/L of PI for 20 min. Nucleus changes in AP, AP-BSA-SeNPs, AP-SA-SeNPs and AP-PET-SeNPs scaffolds were observed using phase contrast microscopy.

5.11. *In vivo* experiment

Healthy male mice (Swiss albino) weighing 28-36 g were used for the study. The experimental procedures followed the guidelines of the Institutional Animal Ethics Committee of India (AKCP/IAEC/72/18-19).

5.12. Grouping of experimental animals and administration of ethanol

The study utilized healthy, disease-free mice, categorizing them into distinct treatment groups as follows:

Group 1: Control (untreated)

Group 2: Ethanol-induced

Group 3: AP hydrogel injected + Ethanol-induced

Group 4: AP-BSA-SeNPs hydrogel injected + Ethanol-induced

Group 5: AP-SA-SeNPs hydrogel injected + Ethanol-induced

Group 6: AP-PET-SeNPs hydrogel injected + Ethanol-induced

In the study, 32% ethanol was orally administered to mice using varying volumes (0.2 to 0.6 ml) via an 18G-sized cannula. This process was done daily or for 30 days to simulate chronic ethanol consumption and assess its effects on the mice.

5.13. Body Weight and Organ Weight Measurements in Treated Groups

The body weights of the treated groups were recorded at intervals on the 1st, 10th, 20th, and 30th days and compared with those of the control group. At the end of the study period, the animals were euthanized, and the vital organ, the heart, was harvested and

placed in a 10% formalin solution. Organ weights, including that of the heart, were also documented.

5.14. Serum Creatine Phosphokinase activity

Serum Creatine Phosphokinase (CPK) activity was assayed as described by Oliver, 1995. A CPK test kit (CK-20; Sigma Chemical Co., St. Louis, MO) based on this method will be used.

6. Results and Discussion

6.1. Antioxidant activity

Studies have indicated that SeNPs possess a strong antioxidant effect that depends on the particles' size [12]. It has been observed that smaller particles have more significant antioxidant activity. The scavenging of free radicals is due to the reduction of methanolic DPPH solution in the presence of a DPPH-H (donate) antioxidant, forming the non-radical form [13]. Antioxidant activity of the SeNPs, BSA-SeNPs, SA-SeNPs, and PET-SeNPs, AP, AP-BSA-SeNPs, AP-SA-SeNPs, and AP-PET-SeNPs scaffolds, CCS, CCS-BSA-SeNPs, CCS-SA-SeNPs, and CCS-PET-SeNPs scaffolds, as well as AP, AP-BSA-SeNPs, AP-SA-SeNPs, and AP-PET-SeNPs hydrogel was observed at 517 nm.

The antioxidant activities of different selenium nanoparticles (SeNPs) were evaluated in this study. SeNPs exhibited an antioxidant activity of 57%. When BSA was coated with SeNPs (BSA-SeNPs) the antioxidant activity increased to 64%. Similarly, surface-modified SeNPs, such as SA-SeNPs and PET-SeNPs, demonstrated 72% and 67% antioxidant activities, respectively. These findings suggest that surface modifications and protein conjugation can significantly enhance the antioxidant properties of selenium nanoparticles.

The AP scaffold alone showed an antioxidant activity of 21%. When conjugated with bovine serum albumin (BSA) and SeNPs (AP-BSA-SeNPs scaffold), the antioxidant activity significantly increased to 62%. The antioxidant activities of the AP scaffold modified with SA-SeNPs and PET-SeNPs were 42% and 40%, respectively. These

results indicate that incorporating SeNPs, particularly with BSA, considerably enhances the antioxidant properties of the AP scaffold.

The CCS scaffold alone exhibited an antioxidant activity of 42%. When the CCS scaffold was conjugated with bovine serum albumin (BSA) and SeNPs (CCS-BSA-SeNPs scaffold), the antioxidant activity increased to 57%. Similarly, the antioxidant activities of the CCS scaffold modified with SA-SeNPs and PET-SeNPs were both 57%. These findings suggest that incorporating SeNPs, whether conjugated with BSA, SA, or PET, uniformly enhances the antioxidant properties of the CCS scaffold.

The AP hydrogel alone demonstrated an antioxidant activity of 68%. When conjugated with bovine serum albumin (BSA) and SeNPs (AP-BSA-SeNPs hydrogel), the antioxidant activity slightly increased to 71%. Similarly, the antioxidant activities of the AP hydrogel modified with SA-SeNPs and PET-SeNPs were 69% and 72%, respectively. These results indicate that incorporating SeNPs, particularly with PET, can slightly enhance the antioxidant properties of the AP hydrogel.

The study concludes that selenium nanoparticles (SeNPs) significantly enhance antioxidant activity, with surface modifications and protein conjugation further amplifying these effects. This suggests SeNPs' potential to boost the selenoenzyme glutathione peroxidase to combat free radical damage in vivo [14,15].

6.2. Morphology of C2C12 cell line in AP and AP-BSA-SeNPs, AP-SA-SeNPs, AP-PET-SeNPs scaffolds

The morphology of the AP scaffold, AP-BSA-SeNPs scaffold, AP-SA-SeNPs scaffold and AP-PET-SeNPs scaffold attaching C2C12 cells were presented in (Fig.2) under phase contrast microscopy (EVOS). The morphology of the C2C12 cells under phase contrast microscopy with AP and AP-BSA-SeNPs, AP-SA-SeNPs, AP-PET-SeNPs scaffolds was shown in (Figure 2a-d). Some studies explored how rough surfaces diminish innate immune reactions and prevent implant rejection after transplantation [16]. The C2C12 cells were grown on AP and AP-BSA-SeNPs, AP-SA-SeNPs and AP-PET-SeNPs scaffolds to demonstrate cell morphology and attachment. Significant

differences in cell density were seen between AP scaffold and the AP-BSA-SeNPs, AP-SA-SeNPs and AP-PET-SeNPs scaffold. This indicates that C2C12 cells can proliferate while cultured on an AP-BSA-SeNPs, AP-SA-SeNPs and AP-PET-SeNPs scaffold.

6.2.1. Evaluation of propidium iodide staining

The C2C12 cells in AP, AP-BSA-SeNPs, AP-SA-SeNPs and AP-PET-SeNPs scaffolds were stained with propidium iodide to visualize nuclei variations. In the cells, the nucleus was circular and there were no significant differences in the AP-BSA-SeNPs, AP-SA-SeNPs and AP-PET-SeNPs scaffolds compared to the control AP scaffold, as shown in (Figure 2e-h).

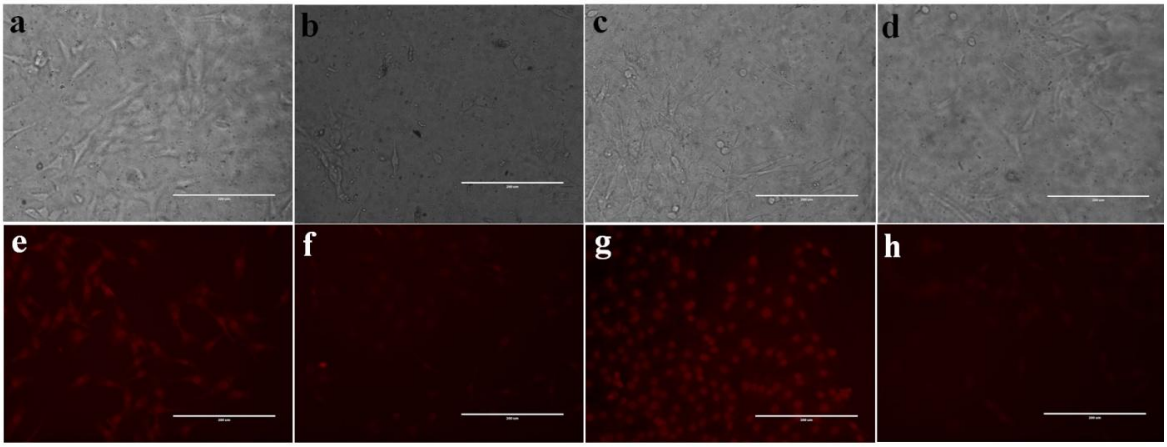

Figure 2. Phase contrast microscopy images of (a) AP scaffold with C2C12 cells at 5th day (b) AP-BSA-SeNPs scaffold with cells at 5th day (c) AP-SAT-SeNPs scaffold with cells at 5th day (d) AP-PET-SeNPs scaffold with cells at 5th day (e-h) Propidium iodide stained with DNA condensation observed by AP, AP-BSA-SeNPs, AP-SAT-SeNPs and AP-PET-SeNPs scaffolds with C2C12 cells on the 5th day.

6.3. Morphology of C2C12 cell line in CCS, CCS-BSA-SeNPs, CCS-SA-SeNPs and CCS-PET-SeNPs scaffolds

Figure 3(a-d) displays the morphological characteristics of C2C12 cells attached to scaffolds, including CCS, CCS-SeNPs, CCS-SA-SeNPs, and CCS-PET-SeNPs. These cell images were captured in fluorescence microscopy (EVOS epifluorescence

microscope). The C2C12 cells were cultivated on CCS, CCS-SeNPs, CCS-SA-SeNPs, and CCS-PET-SeNPs scaffolds to illustrate their attachment and morphology. A notable contrast in cell density was observed between the CCS scaffold and the CCS-SeNPs, CCS-SA-SeNPs, and CCS-PET-SeNPs scaffolds. This observation suggests that C2C12 cells exhibit enhanced proliferation when cultured on CCS-SeNPs, CCS-SA-SeNPs, and CCS-PET-SeNPs scaffolds. These C2C12 cells exhibited a spindle-shaped morphology, and this characteristic remained consistent even after 5 days of culture. Another study [17] reported that the surfaces of polystyrene and polyhydroxybutyrate (PHB) film led to an increased fusion index in C2C12 and H9C2 cell lines when cultured on nanofibrous (nF) substrates. This increase was particularly prominent in aligned nF samples, which remained distinct from other substrates after 3 days of differentiation. For C2C12 cells, no significant differences in myotube length were observed even after 3 days of differentiation across different sample types. In terms of scaffold surface characteristics, it is worth noting that smooth surfaces of scaffolds often induce strong inflammatory reactions, potentially leading to the formation of a fibrotic capsule around the implant. The results indicated that C2C12 cells exhibited more efficient proliferation when cultured on the CCS-SeNPs, CCS-SA-SeNPs and CCS-PET-SeNPs scaffold compared to the CCS scaffold. These findings suggest that the smooth surfaces of the CCS-SeNPs and CCS-PET-SeNPs scaffolds promote enhanced cell attachment and proliferation, which may ultimately contribute to improved tissue regeneration.

6.3.1. Evaluation of nucleus morphology using PI staining

The C2C12 cells in various scaffolds, including CCS, CCS-SeNPs, CCS-SA-SeNPs, and CCS-PET-SeNPs, were stained PI to observe nucleus morphology. The nuclei in all these cells appeared circular, and there were no noteworthy variances compared to the control CCS scaffold, as depicted in Figure 3(e-h). This observation is consistent with the findings in a study by Kalishwaralal et al. [18], where chitosan-SeNPs and chitosan films were used to stain H9C2 cells with propidium iodide. In that study, the nucleus of H9C2 cells exhibited a circular and structurally intact appearance, regardless of the type of film used. The study concluded that incorporating different sizes of SeNPs into chitosan films

did not lead to noticeable changes in ROS production or alterations in nuclear structure in H9C2 cells after 5 days of culture.

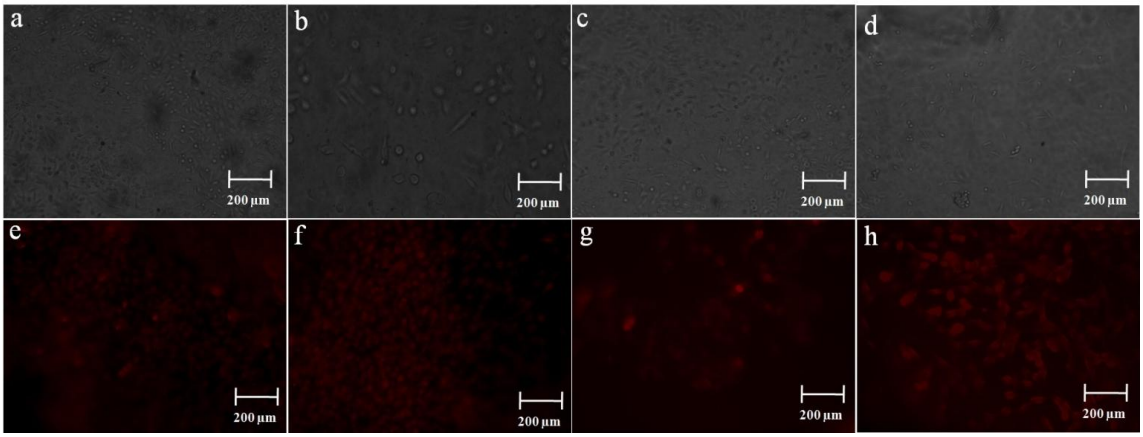

Figure 3. Phase contrast microscopy images of (a-d) CCS, CCS-SeNPs, CCS-SAT-SeNPs and CCS-PET scaffolds with C2C12 cells at 5th day; (e-h) PI stained with DNA condensation observed by CCS, CCS-SeNPs, CCS-SAT-SeNPs and CCS-PET scaffolds with C2C12 cells on the 5th day.

6.4. *In vivo* experiments

6.4.1. Body weight and Organ weight

The study assessed the treatment of various hydrogels on alcoholic cardiomyopathy in mice over 30 days. Ethanol treatment decreased body weights across all groups, with the highest concentration causing the most significant reduction. AP hydrogel injections and different types of SeNPs exacerbated this effect. The study found significant variations in heart weights across experimental groups receiving different ethanol concentrations and hydrogel injections. Mice treated solely with ethanol showed a dose-dependent decrease in heart weight, while those injected with ethanol and various hydrogels demonstrated a dose-dependent increase. Table 1 highlights statistically significant differences in heart organ weight. Notably, mice injected with specific hydrogel formulations showed lighter organ weights than those injected with AP hydrogel, suggesting potential cardioprotective effects against ethanol-induced cardiotoxicity.

Table 1. Comparison of heart weight in mice from the exposed ethanol-induced and hydrogel injected with ethanol-induced group and control

Heart weight (g)					
Concentration (mL)	**Ethanol-induced**	**AP hydrogel**	**AP-BSA-SeNPs hydrogel**	**AP-SA-SeNPs hydrogel**	**AP-PET-SeNPs hydrogel**
Control			**0.11 ± 0.002**		
0.2	**0.16 ± 0.002**	**0.18 ± 0.0036**	**0.12 ± 0.002**	**0.15 ± 0.003**	**0.16 ± 0.003**
0.3	**0.16 ± 0.003**	**0.20 ± 0.004**	**0.13 ± 0.003**	**0.16 ± 0.003**	**0.17 ± 0.003**
0.4	**0.16 ± 0.003**	**0.20 ± 0.004**	**0.16 ± 0.003**	**0.16 ± 0.003**	**0.19 ± 0.004**
0.5	**0.13 ± 0.003**	**0.21 ±0.004**	**0.16 ± 0.003**	**0.21 ±0.004**	**0.19 ± 0.004**
0.6	**0.12 ± 0.003**	**0.21 ± 0.004**	**0.16 ±0.003**	**0.21 ±0.004**	**0.22 ± 0.004**

6.4.2. Comparative Analysis of CPK Enzyme Levels in Treated and Control Groups

The effect on serum CPK level. Because ethanol-induced disrupts the cardiac myocyte membrane, the release of intracellular CPK into serum was used to evaluate the existence and extent of myocyte injury. Ethanol-induced and AP hydrogel treatment (concentration 0.5 and 0.6 ml) resulted in a threefold increase in serum CPK activity compared with the control group (Figure 4). Interestingly, the treatment of AP-BSA-SeNPs hydrogel, AP-PET-SeNPs hydrogel, and AP-PET-SeNPs hydrogel resulted in lighter CPK activity than the control group. The ethanol-induced and injected AP-BSA-SeNPs hydrogel, AP-SA-SeNPs hydrogel, and AP-PET-SeNPs hydrogel-treated mice significantly decreased CPK levels. These results indicate that AP-BSA-SeNPs hydrogel, AP-SA-SeNPs hydrogel, and AP-PET-SeNPs hydrogel reduce ethanol-induced necrosis in mouse hearts.

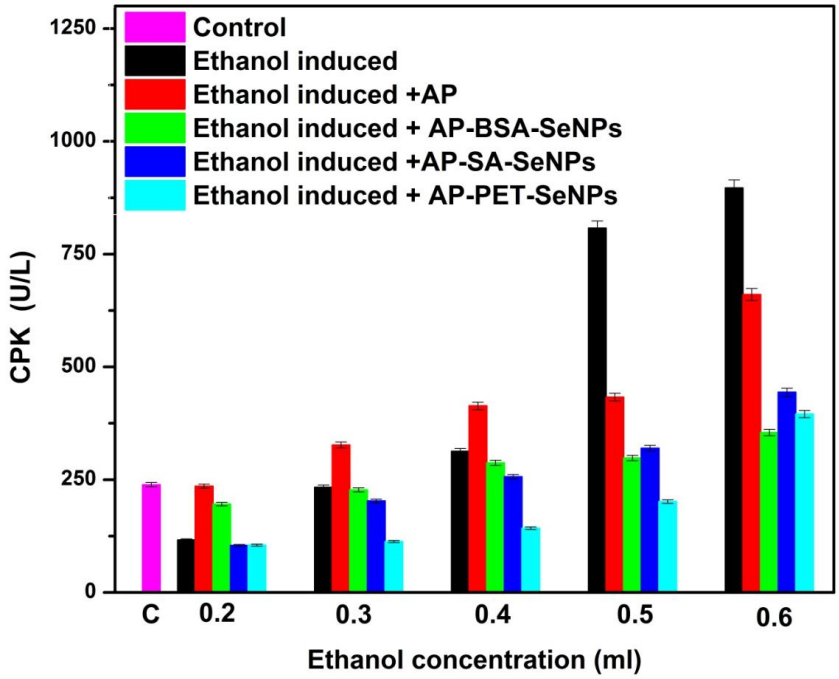

Figure 4. The CPK activities in the ethanol-treated mice and the effect of AP hydrogel, AP-BSA-SeNPs hydrogel, AP-SA-SeNPs hydrogel, and AP-PET-SeNPs hydrogel treatments.

7. Conclusion

The study successfully demonstrated the synthesis of polymer-decorated selenium nanoparticles (SeNPs) using sodium alginate, pectin, and BSA, confirmed through FTIR and XRD analyses. DLS results indicated the nanoparticles were less than 200 nm, ensuring stability and enhanced antioxidant activity. These polymer-decorated SeNPs showed promise as cardiotherapeutic agents at 10 to 20 µg/ml dosages. SEM-EDX analysis confirmed the incorporation of SeNPs into various scaffolds (AP and CCS), which exhibited increased antioxidant activity and improved cell attachment and proliferation of C2C12 cell lines. *In vivo*, SeNP-incorporated AP hydrogels reduced creatine phosphokinase (CPK) levels and improved heart tissue morphology in hydrogel-injected, chronic ethanol-consumed mice. These findings highlight the potential of injectable hydrogels, such as AP-BSA-SeNPs, AP-SA-SeNPs, and AP-PET-SeNPs, in addressing alcohol consumption and related cardiac diseases.

8. References

[1]. M. Chudzińska, Ł. Wołowiec, J. Banach, D. Rogowicz, G. Grześk, Alcohol and Cardiovascular Diseases—Do the Consumption Pattern and Dose Make the Difference?, *Journal of Cardiovascular Development and Disease*, **9** (10) (2022), 317.

[2]. T.S. Leyane, S.W. Jere, N.N. Houreld, Oxidative Stress in Ageing and Chronic Degenerative Pathologies: Molecular Mechanisms Involved in Counteracting Oxidative Stress and Chronic Inflammation, *International Journal of Molecular Sciences*, **23** (13) (2022).

[3]. A. George, V.M. Figueredo, Alcoholic Cardiomyopathy: A Review, *Journal of Cardiac Failure*, **17** (10) (2011), 844–849.

[4]. M.R. Piano, Alcoholic Cardiomyopathy: Incidence, Clinical Characteristics, and Pathophysiology, *Chest*, **121** (5) (2002), 1638–1650.

[5]. R.A. Kloner, S.H. Rezkalla, To Drink or Not to Drink? That Is the Question, *Circulation*, **116** (11) (2007), 1306–1317.

[6]. M.K.M. Kuppari, Alcohol and cardiovascular disease, (2007).

[7]. K.-J. Bär, M.K. Boettger, M. Koschke, S. Boettger, M. Grotelüschen, A. Voss, V.K. Yeragani, Increased QT interval variability index in acute alcohol withdrawal, *Drug and Alcohol Dependence*, **89** (2) (2007), 259–266.

[8]. R.A. Brown, M. Crawford, M. Natavio, P. Petrovski, J. Ren, Dietary magnesium supplementation attenuates ethanol- induced myocardial dysfunction, *Alcoholism: Clinical and Experimental Research*, **22** (9) (1998), 2062–2072.

[9]. N.L. Ihekire, O.E. Okobi, E.A. Adedoye, P.F. Akahara, A.O. Onyekwere, J. Afrifa-Yamoah, F.B. Akinyemi, Heartache in a Bottle: Understanding Alcoholic Cardiomyopathy, *Cureus*, **15** (8) (2023).

[10]. E. Grunvald, R. Shah, R. Hernaez, A.K. Chandar, O. Pickett-Blakely, L.M. Teigen, T. Harindhanavudhi, S. Sultan, S. Singh, P. Davitkov, AGA Clinical Practice Guideline on Pharmacological Interventions for Adults With Obesity, *Gastroenterology*, **163** (5) (2022), 1198–1225.

[11]. T.-C. Ho, C.-C. Chang, H.-P. Chan, T.-W. Chung, C.-W. Shu, K.-P. Chuang, T.-H. Duh, M.-H. Yang, Y.-C. Tyan, Hydrogels: Properties and applications in biomedicine, *Molecules*, **27** (9) (2022), 2902.

[12]. S.K. Torres, V.L. Campos, C.G. León, S.M. Rodríguez-Llamazares, S.M. Rojas, M. González, C. Smith, M.A. Mondaca, Biosynthesis of selenium nanoparticles by Pantoea agglomerans and their antioxidant activity, *Journal of Nanoparticle Research*, **14** (11) (2012), 1236.

[13]. A. Wan, Q. Xu, Y. Sun, H. Li, Antioxidant Activity of High Molecular Weight Chitosan and N,O-Quaternized Chitosans, *Journal of Agricultural and Food Chemistry*, **61** (28) (2013), 6921–6928.

[14]. A.-M.E. Abdel-Moneim, M.T. El-Saadony, A.M. Shehata, A.M. Saad, S.A. Aldhumri, S.M. Ouda, N.M. Mesalam, Antioxidant and antimicrobial activities of Spirulina platensis extracts and biogenic selenium nanoparticles against selected pathogenic bacteria and fungi, *Saudi Journal of Biological Sciences*, **29** (2) (2022), 1197–1209.

[15]. N. Shahabadi, S. Zendehcheshm, F. Khademi, Selenium nanoparticles: Synthesis, in-vitro cytotoxicity, antioxidant activity and interaction studies with ct-DNA and HSA, HHb and Cyt c serum proteins, *Biotechnology Reports*, **30** (2021), e00615.

[16]. L. Meinel, S. Hofmann, V. Karageorgiou, C. Kirker-Head, J. McCool, G. Gronowicz, L. Zichner, R. Langer, G. Vunjak-Novakovic, D.L. Kaplan, The inflammatory responses to silk films in vitro and in vivo, *Biomaterials*, **26** (2) (2005), 147–155.

[17]. L. Ricotti, A. Polini, G.G. Genchi, G. Ciofani, D. Iandolo, H. Vazão, V. Mattoli, L. Ferreira, A. Menciassi, D. Pisignano, Proliferation and skeletal myotube formation capability of C2C12 and H9c2 cells on isotropic and anisotropic electrospun nanofibrous PHB scaffolds, *Biomedical Materials*, **7** (3) (2012), 35010.

[18]. K. Kalishwaralal, S. Jeyabharathi, K. Sundar, S. Selvamani, M. Prasanna, A. Muthukumaran, A novel biocompatible chitosan–Selenium nanoparticles (SeNPs) film with electrical conductivity for cardiac tissue engineering application, *Materials Science and Engineering: C*, **92** (2018), 151–160.

List of Publication from this work

1. **S. Naveenkumar**, N. Venkateshan, K. Kaviyarasu, J.R.S.S. Christyraj, A. Muthukumaran, Optimum performance of a novel biocompatible scaffold comprising alginate-pectin-selenium nanoparticles for cardiac tissue engineering using C2C12 cells, *Journal of Molecular Structure*, **1294** (2023), 136457.
2. **S. Naveenkumar**, N. Alagumanikumaran, K. Kaviyarasu, A. Muthukumaran, Influence of encapsulated sodium alginates and pectin on selenium nanoparticles and efficient cardioprotective effect in C2C12 cell line, *Journal of Nanoparticle Research*, **26** (3) (2024), 52.
3. **S. Naveenkumar**, Johnson Retnaraj Samuel Selvan Christyraj, K. Kaviyarasu, A. Muthukumaran, A novel BSA-coated nano selenium-impregnated scaffold showed improved strength, cellular attachment and proliferation in C2C12 cell, *Journal of King Saud University - Science*, **36** (2024),103307.